AMERICAN SOCIETY of
GENE & CELL
THERAPY

rAAV2-Retro Enables Extensive and High-Efficient Transduction of Lower Motor Neurons following Intramuscular Injection

Zhilong Chen,[1,2] Guoqing Fan,[1,2] Anan Li,[1,2] Jing Yuan,[1,2] and Tonghui Xu[1,2,3]

[1]Britton Chance Center for Biomedical Photonics, Wuhan National Laboratory for Optoelectronics, Huazhong University of Science and Technology, Wuhan, China; [2]MoE Key Laboratory for Biomedical Photonics, Collaborative Innovation Center for Biomedical Engineering, School of Engineering Sciences, Huazhong University of Science and Technology, Wuhan, China; [3]Institute of Life Sciences, Nanchang University, Nanchang, China

The motor system controls muscle movement through lower motor neurons in the spinal cord and brainstem. Lower motor neurons are efferent neurons in the central nervous system (CNS) characterized by axonal projections that reach specific targets in the periphery. Lower motor neuron lesions result in the denervation and dysfunction of peripheral skeletal muscle. Great progress has been made to develop therapeutic strategies to transduce lower motor neurons with genes. However, the widespread distribution of lower motor neurons makes their specific, extensive, and efficient transduction a challenge. In this study, we demonstrated that, compared to the other tested recombinant adeno-associated virus (rAAV) serotypes, rAAV2-retro mediated the most efficient retrograde transduction of lower motor neurons in the spinal cord following intramuscular injection in neonatal mice. A single injection of rAAV2-retro in a single muscle enabled the efficient and extensive transduction of lower motor neurons in the spinal cord and brainstem rather than transducing only the lower motor neurons connected to the injected muscle. rAAV2-retro achieved the extensive transduction of lower motor neurons by the cerebrospinal fluid pathway. Our work suggests that gene delivery via the intramuscular injection of rAAV2-retro represents a promising tool in the development of gene therapy strategies for motor neuron diseases.

INTRODUCTION

Motor neurons located in the cortex, brainstem, or spinal cord are neural circuit nodes for the motor system to control the behavior of organisms.[1,2] There are two types of motor neurons: upper motor neurons and lower motor neurons. Lower motor neurons are located mainly in the spinal cord or the motor nuclei of the brainstem, and their axons project directly to effectors outside the central nervous system (CNS), mainly muscles and glands, representing the "final common pathway."[3] When a motor command is issued, lower motor neurons produce a divergent motor output, coordinating multiple muscles to achieve movement. Lower motor neurons are segmental; for example, the upper and lower limbs are controlled by the lower motor neurons in the cervical segment and the lumbar segment, respectively.[4] When genetic defects are present in lower motor neu-

rons, such as in spinal muscular atrophy, motor dysfunction arises, thus affecting the quality of life of the individual.[5] Unfortunately, available drug- and biological-based therapeutic strategies are inadequate to treat or cure motor neuron diseases. In recent years, gene therapy involving the transduction of genes into lower motor neurons as a suitable alternative to treating motor neuron diseases has received great attention from clinicians and scientists working on several models of these diseases.[6–8]

Thus far, the most specific and ideal gene therapy strategy for treating motor neuron diseases is the axonal retrograde transduction of motor neurons in the spinal cord through neuromuscular junctions following intramuscular injection.[9] Following peripheral injection, viral-mediated transgenes ideally undergo retrograde transport to the motor neurons in the spinal cord.[10–12] In this regard, recombinant adeno-associated virus (rAAV) therapy, which offers the possibility of expressing a therapeutic gene in a long-term manner, has been used in animal models of motor neuron diseases with promising outcomes.[8,13] As a replication-defective virus, rAAV is capable of long-term latencies in mammalian cells and is therefore considered safe for use in virus-mediated human gene therapy.[14] Recently, phase 1 clinical trials using rAAV gene therapy for pediatric spinal muscular atrophy and giant axonal neuropathy have begun,[15,16] Many attempts have been made to retrogradely transduce the CNS by injecting rAAV into muscles.[8,10,11] Despite progress, the distribution of lower motor neurons is broad, and lower motor neurons are located in the deep ventral horn of the spinal cord, which makes the extensive and efficient transduction of lower motor neurons a challenge.

The development of rAAV2-retro, a newly evolved variant with robust retrograde transduction properties,[17] offers new opportunities to address this challenge. rAAV2-retro has been widely used for retrograde labeling in the CNS, such as the brain and spinal cord.[18,19] However, the retrograde transduction efficiency of peripheral injection remains unknown. In this study, we compared eight commercially available rAAV serotypes as tools to transduce lower motor neurons through intramuscular injection in neonatal mice. First, we found that rAAV2-retro transduced the lower motor neurons of the cervical spinal cord more efficiently than did the other tested rAAV serotypes. Moreover, the detailed visualization of rAAV2-retro-transduced motor neurons revealed the extensive transduction of lower motor neurons, not just of the lower motor neurons that project into the injected muscle. By using CTB conjugated to Alexa Fluor 647 (CTB-647) coinjection for normalization, we found that the lower motor neurons projecting to the injected muscle were transduced with 57% efficiency, with robust transgene expression within 6 days after injection. Finally, we determined that the extensive transduction of lower motor neurons by rAAV2-retro occurred through the cerebrospinal spinal fluid diffusion pathway. In general, these data highlight the promising application of rAAV2-retro intramuscular injection in neuroanatomical studies and in gene delivery for the treatment of motor neuron diseases.

RESULTS

Comparison of the Retrograde Transduction Efficiency of rAAVs in Cells in the Ipsilateral Spinal Cord

First, we compared the retrograde transduction efficiency of rAAV2-retro with that of the other seven commercially available rAAV serotypes (rAAV1, rAAV2, rAAV5, rAAV6, rAAV7, rAAV8, and rAAV9) in the spinal cord following intramuscular injection. All of the rAAV serotypes expressed the GFP protein under the control of the cytomegalovirus (CMV) promoter and were injected into the right forelimb *extensor carpi radialis* of mice on postnatal day 4 (P4) (Figure S1). The tested rAAVs contained different capsids, but their genomes contained the same terminal repeats derived from rAAV2. To minimize the individual differences among the rAAV infections, we injected the rAAV serotypes into the *extensor carpi radialis* at a standardized site in the right forelimb of each mouse. The exact injection site was determined by the trend of the blood vessels.

The *extensor carpi radialis* is innervated by the radial nerve, which receives projections from ipsilateral spinal cord levels C5, C6, C7, C8, and T1.[20,21] In addition, intramuscular injection based on fluorescent gold indicated that *extensor carpi radialis* receives projections between segments C2 and C7 of ipsilateral cervical spinal cord in mice.[22] In summary, the cervical segments for the motor columns should be located between C2 and T1. Therefore, we compared the efficiency of rAAV vector-mediated retrograde transduction in the cells in the ipsilateral cervical spinal cord 4 weeks after the intramuscular injection of an rAAV vector. All rAAVs induced the retrograde labeling of cells in the corresponding cervical spinal cord levels (Figures 1A–1H). Of the eight tested vectors, rAAV2-retro resulted in the highest number of GFP-positive cells in the ipsilateral spinal cord

(Figures 1H–1J, p < 0.001). The results showed that all rAAV serotypes affected the cells in the spinal cord following intramuscular injection and that rAAV2-retro mediated the most efficient retrograde transduction.
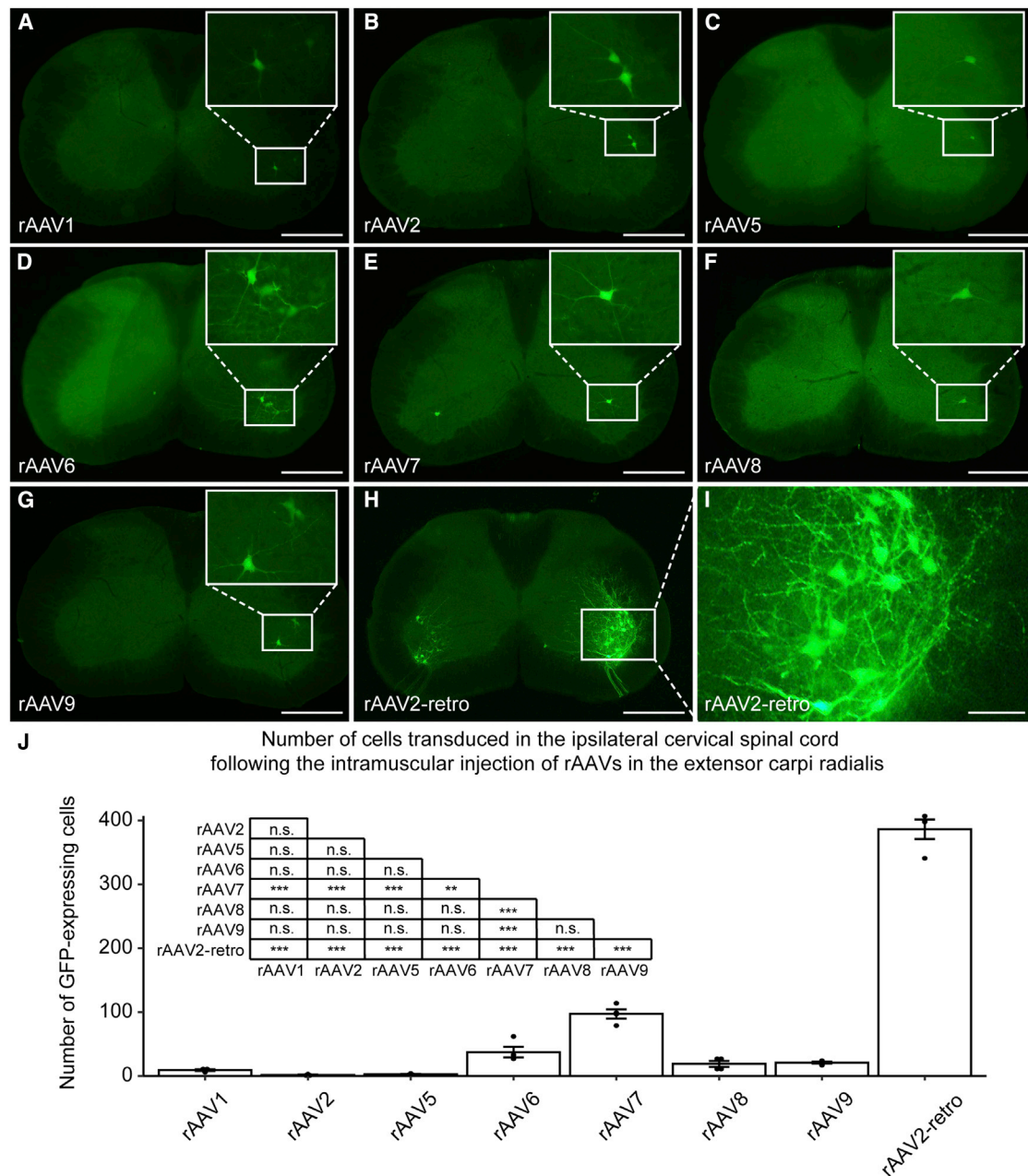
Comparison of the Retrograde Transduction Efficiency of rAAVs in Cells in the Contralateral Spinal Cord

During the analysis of the retrograde efficiency of the rAAVs, we found a large number of GFP-positive cells in the contralateral cervical spinal cord after the intramuscular injection of rAAV2-retro (Figure S2A). Of all the transduced cells in the cervical spinal cord, 387.2 ± 15.4 cells were located on the ipsilateral side, and 188.3 ± 14.7 cells were located on the contralateral side (Figure S2B, p < 0.001). Therefore, those in the contralateral cervical spinal cord accounted for 32.5% ± 1.0% of all the GFP-positive cells in the cervical spinal cord. To further analyze the efficiency of retrograde transduction to the bilateral spinal cord after the intramuscular injection of rAAV2-retro, we measured the maximum fluorescence intensity of the GFP-positive cells on both sides of the same spinal cord section, and the results showed that the fluorescence in the ipsilateral ventral horn of the cervical spinal cord was 103.47 ± 3.30 a.u. and that the fluorescence in the contralateral ventral horn of the cervical spinal cord was 47.92 ± 2.49 a.u. (Figure S2C, p < 0.001). Of the other tested rAAV serotypes, we also found that rAAV7, rAAV8, and rAAV9 were able to transduce sporadic cells in the contralateral cervical spinal cord but were significantly less efficient than rAAV2-retro (Figure S2D–S2F). Our data suggest that rAAV2-retro can retrogradely infect both sides of the spinal cord after intramuscular injection, while the efficiency of retrograde transport to the contralateral spinal cord was significantly lower than that to the ipsilateral spinal cord.

Widespread Distribution of rAAV2-Retro-Transduced Cells in the CNS

Previous research has shown that scAAV9 mediates widespread gene delivery to the spinal cord following intramuscular injection.[8,13] In this study, our data show that the unilateral intramuscular injection of rAAV2-retro retrogradely transduces cells in the contralateral spinal cord, suggesting that intramuscular rAAV2-retro injection may mediate the widespread transduction of cells throughout the CNS. To explore the three-dimensional cellular localization and distribution of the transduced cells, we administered a single injection of rAAV2-retro to the right forelimb *extensor carpi radialis* in P4 neonatal mice and then performed FDISCO (DISCO with superior fluorescence preserving capability) tissue clearing of the whole spinal cord (Figure 2; Video S1) and the whole brain (Figure 3) after 4 weeks. For better visualization, we doubled the titer of rAAV2-retro to counteract the compromising effect of the clearing reagent on the fluorescence protein signal.

As shown in Figures 2A–2E, the rAAV2-retro-transduced cells were arranged linearly along the bilateral ventral horn of the spinal cord. The caudal vertebra was merged into the sacral vertebra due to

Figure 1. Comparison of the Transduction Efficiency after the Intramuscular Delivery of Eight Serotypes of rAAV

(A–H) Native GFP-expressing cells in transverse cervical spinal cord sections following retrograde transport with recombinant adeno-associated virus (rAAV)-CMV-GFP injection to *extensor carpi* muscle of the right forelimb of P4 mice (scale bars, 500 μm). (A) rAAV1, (B) rAAV2, (C) rAAV5, (D) rAAV6, (E) rAAV7, (F) rAAV8, (G) rAAV9, and (H) rAAV serotype retro (rAAV-retro). (I) Magnification of (H) (scale bar, 100 μm). (J) Total number of native GFP-expressing cells in the ipsilateral cervical spinal cord. rAAV2-retro demonstrates significantly more efficient retrograde infection than do other serotypes. Statistical analysis of fluorescence measurements is shown in the bar graphs. $**p < 0.01$, $***p < 0.001$, one-way ANOVA followed by the Bonferroni correction (error bars indicate mean ± SEM; n = 4/group). n.s., not significant.

blurred boundaries during visualization. Meanwhile, to reduce the possibility of virus leakage, we reduced the injection volume to 0.5 μL and increased the titer to 1×10^{14} genome copies/mL, which also obtained extensive transduction results, and the results of the labeled cells were marked for counting and location statistics. Moreover, the distribution patterns of the cells in the bilateral ventral horn of the spinal cord were similar (Figure 2F). There were two dense distributions in the cervical and lumbar spinal cord, which correspond to
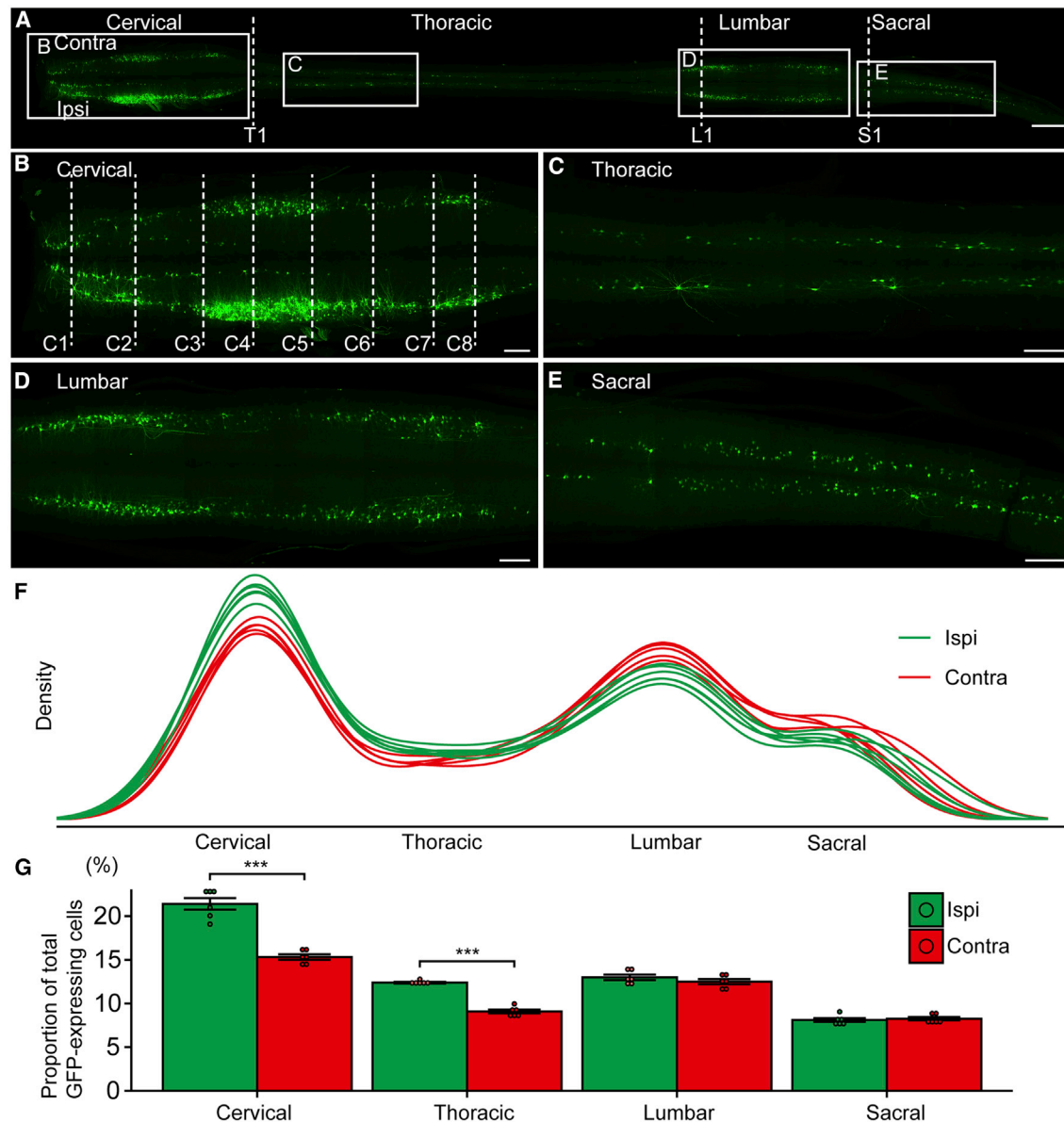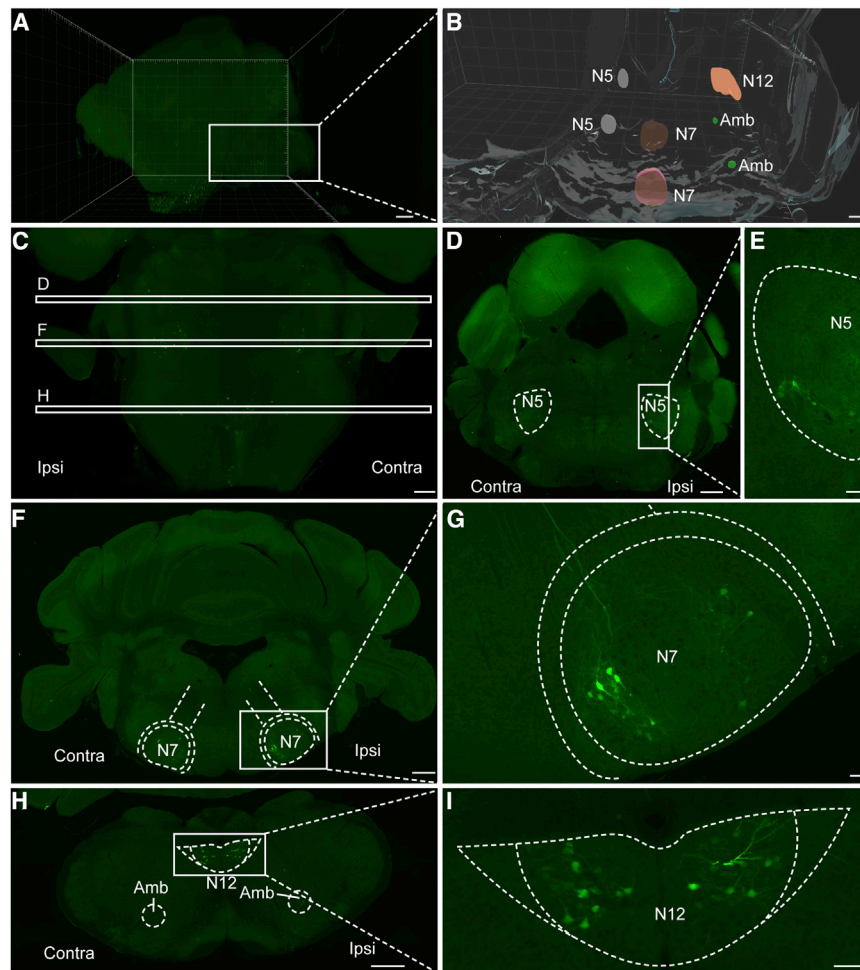
Figure 2. Intramuscular Injection of rAAV2-Retro Extensively Transduced Cells in the Spinal Cord

(A) Visualization of the whole spinal cord confocal imaging for mice injected into the right *extensor carpi* muscle with rAAV2-retro-CMV-GFP after whole spinal cord FDISCO clearing (scale bars, 1,000 μm). (B–D) Enlarged horizontal views of cervical (B), thoracic (C), lumbar (D), and sacral spinal cord (E) as in (A), respectively (scale bars, 200 μm). (F) Density maps of cells along the anterior-posterior axes of spinal cord. (G) Quantification of GFP-positive cells by percentile in four different spinal cord levels of each side. ***p < 0.001, independent-sample t test (two-sided) (error bars indicate mean ± SEM). Contra, contralateral side; Ipsi, ipsilateral side.

the cervical and lumbar enlargements of the spinal cord. In the cervical spinal cord, the labeled cells on the ipsilateral side were much denser than those on the contralateral side. Quantitatively, more cells were transduced in the ipsilateral cervical and thoracic spinal cord than in the contralateral cervical and thoracic spinal cord, while there was no difference between the different sides of the lumbar and sacral spinal cord (Figure 2G). As the distance from the injection site increased, the number of transduced cells on both sides of the spinal

cord, for example, in the lumbar and sacral spinal cord, tended to be consistent. We performed the same experiment and injected rAAV2-retro-CMV-red fluorescent protein (RFP) purchased from the same vendor into the gastrocnemius muscle and similarly achieved the extensive transduction of cells (Figure S3). These results indicate that a single intramuscular injection of rAAV2-retro, whether in forelimb or hindlimb muscles, can extensively transduce cells. In addition, the rAAV2-retro-CMV-RFP and rAAV2-retro-CMV-GFP viruses

Figure 3. Intramuscular Injection of rAAV2-Retro Extensively Transduced Cells in the Brainstem

(A) 3D visualization of the intact brain light-sheet imaging for mice injected into the right *extensor carpi* muscle with rAAV2-retro-CMV-GFP after intact brain FDISCO clearing (scale bar, 500 μm). (B) Brainstem model for three-dimensional reconstructions. Depicted are the GFP-expressing structures of cranial motor nuclei N5, N7, N12, and *nucleus ambiguous* (Amb) (scale bar, 500 μm). (C) Enlarged horizontal views of the boxed region in (A) and illustration of the anatomical localization of coronal section (D, F, and H) (scale bar, 500 μm). (D) Representative coronal brain section of N5 (scale bar, 500 μm). (E) Enlarged view of the boxed region in (D) (scale bar, 100 μm). (F) Representative coronal brain section of N7 (scale bar, 500 μm). (G) Enlarged view of the boxed region in (F) (scale bar, 100 μm). (H) Representative coronal brain section of N12 and Amb (scale bar, 500 μm). (I) Enlarged view of the boxed region in (H) (scale bar, 100 μm). Contra, contralateral side; Ipsi, ipsilateral side.

extensively by a single injection of rAAV2-retro in a single muscle in neonatal mice.

Identification of the Cell Types of the rAAV2-Retro Transduced Cells

The above data show that the overall distribution patterns of the transduced cells in the bilateral ventral horn of the spinal cord and in some motor nuclei of the brainstem show a high degree of similarity and are similar to the distribution pattern of lower motor neurons,[1,22,23] To determine whether the transduced cells were lower motor neurons, we used choline acetyltransferase (ChAT) as a marker for cholinergic lower motor neurons. The results showed that all GFP-expressing cells in the ventral horn of the spinal cord and the motor nuclei of the brainstem were labeled with antibodies against ChAT (Figure 4; Figure S4), indicating that the expression of the viral vector in the spinal cord and brainstem was specific to lower motor neurons.

Widespread Distribution of rAAV2-Retro-Transduced Cells in the Dorsal Root Ganglia

As illustrated in Figure S5A, mice injected with the rAAV2-retro-CMV-EGFP at P4 show a moderate level of transduction of nerve fibers in the dorsal horn, including the *fasciculus gracilis* and *fasciculus cuneatus*. Combining with tissue clearing and 3D reconstruction, the nerve fibers of the dorsal horn are derived from the aggregating fibers of all segments of the spinal cord (Figures S5B S5C). Extensive transduction of cells in the dorsal root ganglia (DRGs) were observed following intramuscular injections with rAAV2-retro in P4 neonatal mice (Figure S5D). Trigeminal ganglia neurons were robust retrograde transduced by rAAV2-retro (Figures S5E and S5F). These

were from different batches of viruses from the same vendor, pointing to the differences in the ability to transduce cells in the spinal cord between viral batches or packaged genes.

Unexpectedly, rAAV2-retro administered by intramuscular injection also induced cell transduction in the brainstem (Figures 3A–3C). By reconstructing GFP signals in the brainstem, we found that the transduced cells were located in motor nuclei N5, N7, N12, and *nucleus ambiguus* (Amb) (Figure 3B) in the brainstem. Among the N5 region, the transduced cells were concentrated in the lower part (Figures 3D and 3E). In the N7 brain region, the transduced cells were arranged in a circle in the coronal plane, but very few or no transduced cells were present in the center (Figures 3F and 3G). In the coronal plane of the N12 brain region, the transfected cells were distributed on both sides in a butterfly pattern (Figures 3H and 3I). Transduced cells were sparse in the Amb, which is a major efferent nucleus of the vagus nerve (cranial nerve X) (Figure 3H).

These results suggest that cells in the bilateral ventral horn of the spinal cord and some motor nuclei in the brainstem are transduced
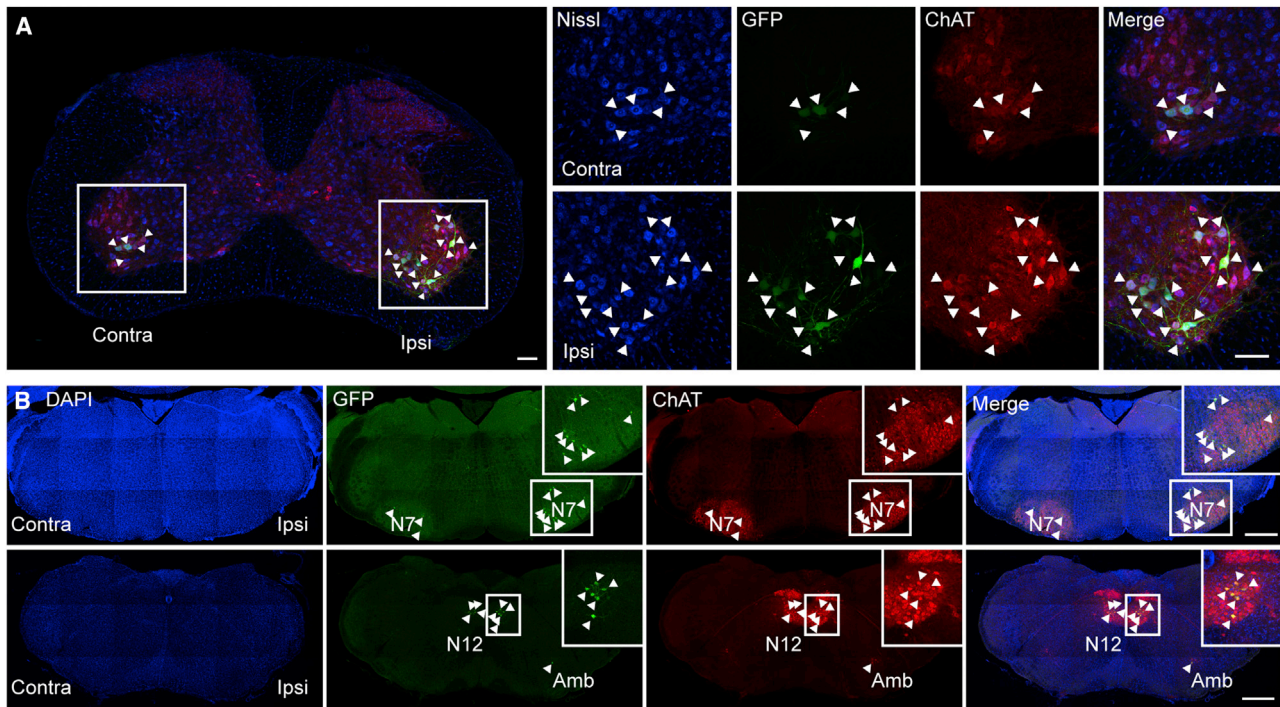
Figure 4. ChAT Antibody Staining of Cells Transduced by rAAV2-Retro

(A) Double-labeled spinal cord sections demonstrating GFP expression in choline acetyltransferase (ChAT)-immunoreactive motor neurons. Blue, Nissl; green, GFP; red, ChAT (arrowheads; scale bars, 200 μm in the upper panel and 100 μm in the lower panel). (B) Double-labeled brainstem sections demonstrating GFP expression in ChAT-immunoreactive motor neurons. Blue: DAPI, green: GFP, red: ChAT (arrowheads; scale bars, 500 μm).

data suggest that rAAV2-retro enables extensive transduction of cells in the dorsal root ganglia.

Quantification of rAAV2-Retro Transduction Efficiency

Although the neuronal transduction of rAAV2-retro was more extensive than that of the other tested rAAVs, its efficiency needs to be further determined. As a retrograde transduction efficiency indicator, cholera toxin subunit B (CTB), is a widely used as a retrograde tracer to efficiently label lower motor neurons that correspond to specific muscles following intramuscular injection.[11,24,25] To comprehensively profile the transduction efficiency of rAAV2-retro in the spinal cord, mice were injected with a mixture of rAAV2-retro-GFP and the retrograde tracer CTB-647 at a single site of the *extensor carpi radialis* in the right forelimb. To avoid the toxic effects of CTB-647 on neurons, the animals were sacrificed just 6 days after injection. The whole spinal cord was imaged by confocal microscopy, and the transduction efficiency was quantified by determining the percentage of CTB-647-positive lower motor neurons in ventral horn of the spinal cord that project to the injected muscle and coexpress GFP (Figure 5A–5C). Virally expressed GFP was expressed in more than 57.04% ± 4.01% of the CTB-647-positive motor neurons by just 6 days postinjection (Figures 5D and 5E). These data demonstrate that rAAV2-retro is highly efficient in the retrograde transduction of lower motor neurons that project to the injected muscle.

To analyze the location bias of the rAAV2-retro-transduced cells, we derived cell position information from three-dimensional coordinates and compared it to the anterior-posterior (A-P), medial-lateral (M-L), or dorsal-ventral (D-V) axes. The rAAV2-retro-transduced cells and CTB-labeled cells showed a distinct location bias, not only at different A-P spinal cord levels (Figure 5F–5H), but also along the M-L and D-V axes (Figures 5I–5L). For example, along the A-P axis, although both populations of cells exhibited two density peaks, the rAAV2-retro-transduced neurons tended to approach the anterior side of the two peaks. Along the M-L and D-V axes, compared to CTB-647, rAAV2-retro had a higher probability of transducing the lateral and ventral neurons. Taken together, these results indicate that rAAV2-retro has a greater probability of transducing lower motor neurons located in the anterior, ventral, and lateral spinal cord.

Determination of the rAAV2-Retro Transduction Pathway

We next explored the mechanism by which rAAV2-retro is extensively transported to the spinal cord and the brainstem following intramuscular injection. We speculated that rAAV2-retro achieves widespread distribution by spreading to the blood or cerebrospinal fluid. In this study, we extracted the cerebrospinal fluid from the lumbar spine or blood from the heart of P4 mice 3 h after the intramuscular injection of rAAV2-retro and used proteinase K to expose the rAAV-packaged DNA fragment. The DNA fragment was verified by PCR to determine the presence of the genes encoding the
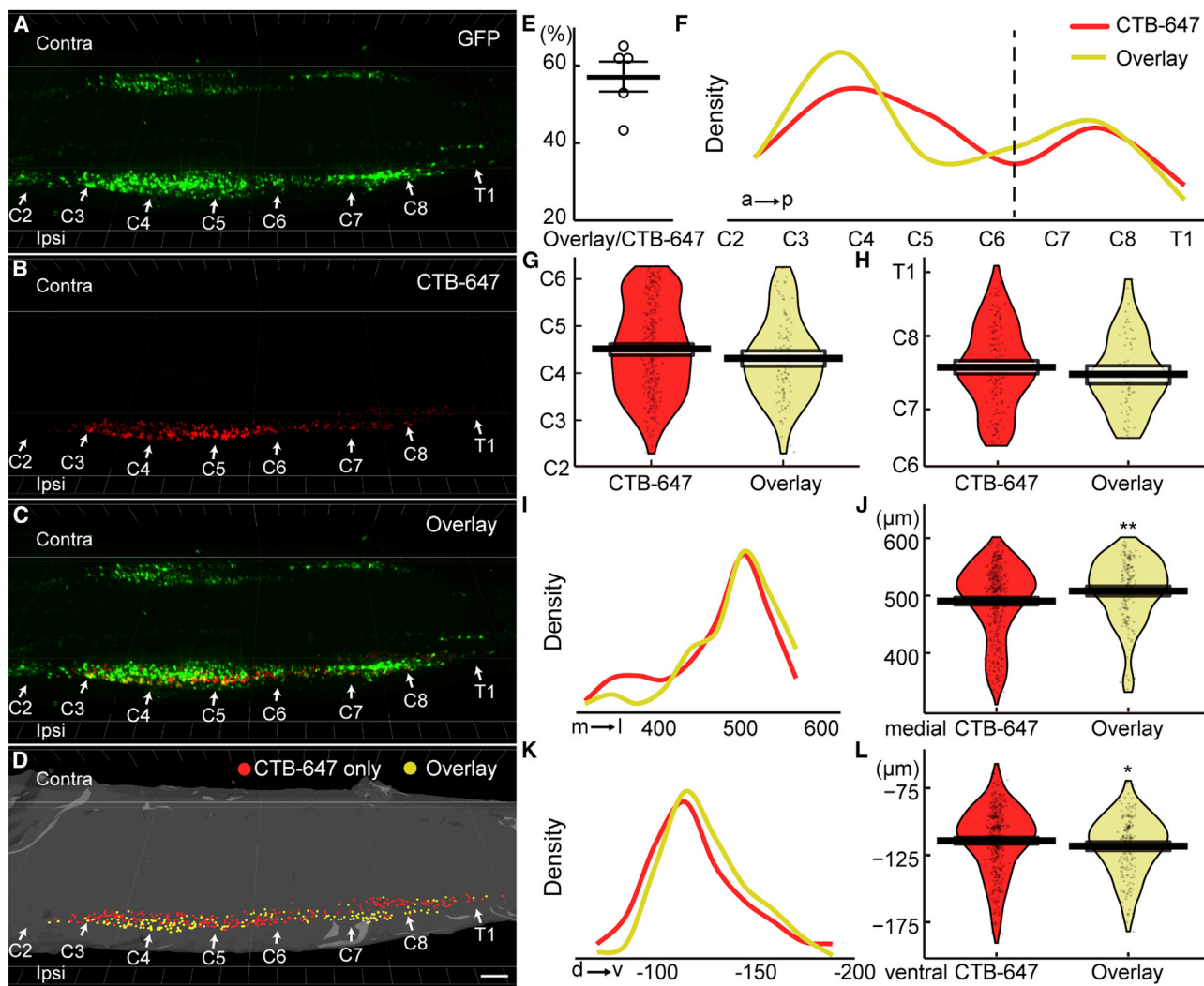
Figure 5. Topographic Distribution of Lower Motor Neurons Co-transduced by rAAV2-Retro and CTB-647 in the Cervical Spinal Cord

(A–D) Three-dimensional imaging of the cervical spinal cord, including the motor neuron pool labeled with AAV2-retro-CMV-GFP (A), cholera toxin B-Alexa Fluor 647 (CTB-647) (B), overlay (C), and isosurface reconstruction: all CTB-647-positive lower motor neurons were identified and marked as red dots in three-dimensional space, after which cell body signals in the corresponding GFP channel were examined and red dots were replaced with yellow dots when they existed (red, CTB only; yellow, overlay) (D) (scale bar, 200 μm). (E) Quantification of GFP detection (overlay) in CTB-647-positive motor neuron bodies. (F, I, and K) Density maps of motor neurons along the anterior-posterior (a-p) (F), medial-lateral (m-l) (I), and dorsal-ventral (d-v) (K) axes of the cervical spinal cord. The units in (I) and (K) equal μm. (G, H, J, and L) Quantification of neurons in different spinal cord levels at C1–C5 (G), C6–C8 (H), and m-l (J) and d-v (L) positions is shown. **p < 0.01, *p < 0.05, independent-sample t test (two-sided). Vertical bars represent the central tendencies, and rectangle represent 95% confidence interval. Contra, contralateral side; Ipsi, ipsilateral side.

fluorescent proteins GFP and RFP. As shown in Figures 6A–6C, rAAV2-retro particles were obviously detected in the cerebrospinal fluid and blood. To further validate the transduction pathway in rAAV2-retro transduction, we implemented the spinal cord transection injury (SCI) model before intramuscular injection. After SCI or sham surgery was completed, rAAV2-retro was injected into the gastrocnemius muscle. After the morphological anatomy, three-dimensional reconstruction, and H&E staining of the spinal cord, the results showed that the lesion epicenter was hollow (Figures 6D–6F). In the ipsilateral thoracic spinal cord, the number of trans-

duced neurons was dependent on the location where the injury was induced, and more neurons were transduced near the posterior side, while few neurons were transduced on the anterior side (Figure 6E). Although there are individual differences in the SCI model, the number and intensity of transduced neurons in the SCI group and sham control group were comparable in the ipsilateral lumbar spinal cord (Figure 6G; Figure S6). In the cervical spinal cord, the SCI group exhibited significantly fewer transduced neurons than that in the sham control group. As SCI did not affect the blood circulatory system of the cervical spinal cord but significantly affected the
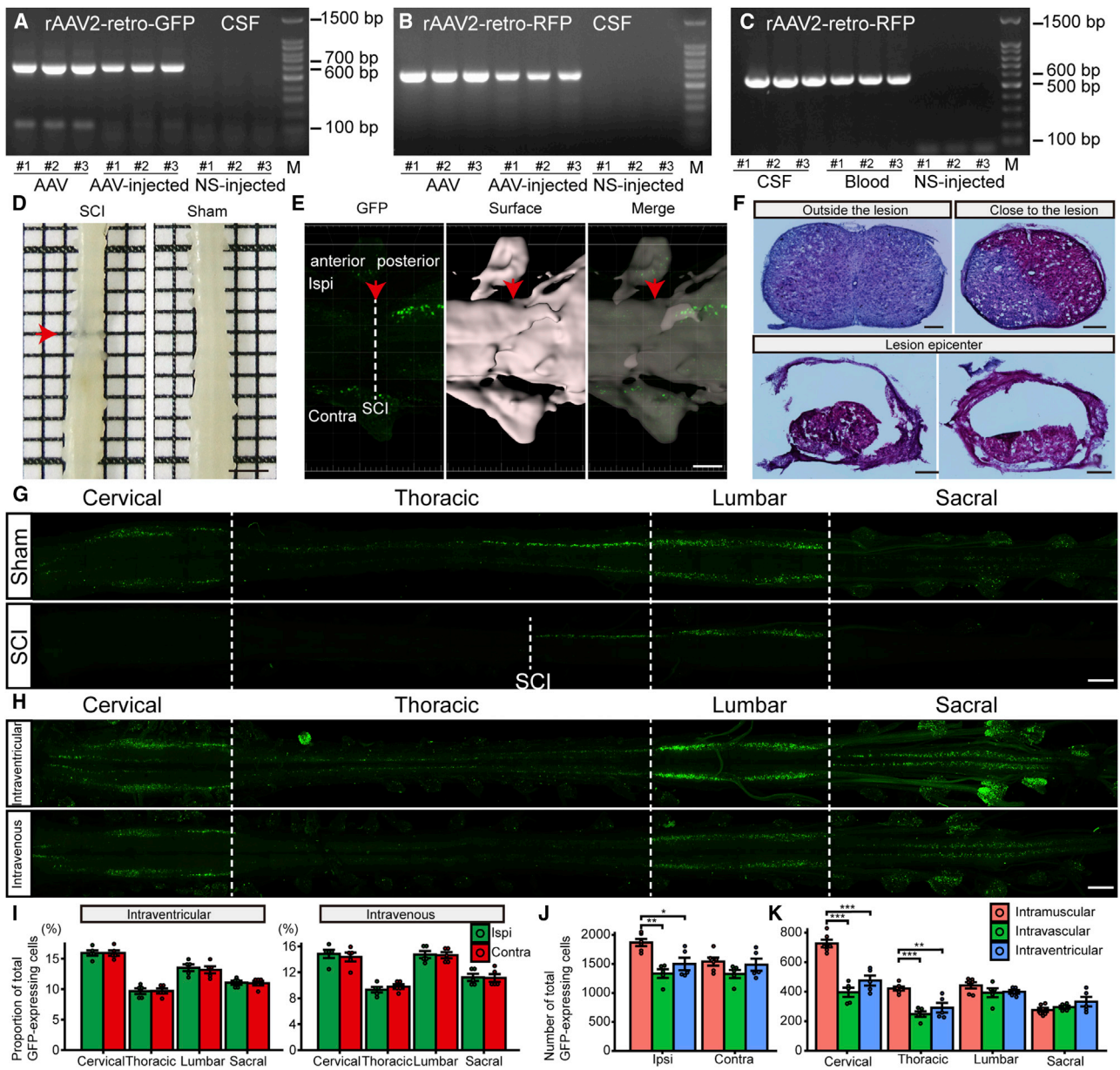
Figure 6. Determination of rAAV2-Retro Transduction Pathway to Spinal Cord Following Intramuscular Injection

(A and B) Cerebrospinal fluid and blood PCR to detect rAAV2-retro, normal saline (NS)-inject: cerebrospinal fluid from mice intramuscularly injected with NS as negative controls. (A) rAAV2-retro-GFP. (B) rAAV2-retro-RFP. (C) Cerebrospinal fluid and blood PCR to detect rAAV2-retro from mice intramuscularly injected with rAAV2-retro. CSF, cerebrospinal fluid. (D) Spinal cords after spinal cord transection injury (SCI) model or sham surgery (red arrow, SCI; scale bar, 2 mm). (E) Surface reconstruction was performed on the lesion area (red arrow, SCI; scale bar, 200 μm). (F) H&E staining was performed on the spinal cord section after SCI (scale bars, 200 μm). (G) Distributions of lower motor neurons transduced after SCI model or sham surgery (scale bar, 500 μm). (H) Distributions of lower motor neurons transduced after intraventricular injection (upper) or intravenous injection (lower) (scale bar, 500 μm). (I) Quantification of GFP-positive cell percentiles in four different spinal cord levels of each side after intraventricular injection (left) or intravenous injection (right). (J) Comparison of the number of cells transduced in spinal cord of each side by three injection routes. (K) Comparison of the number of cells transduced in four different spinal cord levels of ipsilateral side by three injection routes. *$p < 0.05$, **$p < 0.01$, ***$p < 0.001$, one-way ANOVA followed by the Bonferroni correction; error bars represent mean ± SEM. Contra, contralateral side; Ipsi, ipsilateral side.

distribution pattern of the transduced neurons, these results suggest that the extensive transduction of rAAV2-retro in the CNS was achieved by spreading to the cerebrospinal fluid pathway. In addition, neurons in the ipsilateral thoracic segments near the lumbar spine can still be strongly transduced after SCI, which may be achieved by the virus spreading directly through the spinal nerves into the

cerebrospinal fluid. Similarly, extensive transduction of spinal cord neurons was achieved by injecting rAAV2-retro virus into the lateral ventricle (Figure 6H). To verify the role of blood diffusion in the extensive transduction of spinal cord neurons, we injected the temporal vein of P4 mice with rAAV2-retro virus, resulting in transduced neurons in each segment of the spinal cord, and the three-dimensional locations were consistent with those after intramuscular injection (Figure 6H). These results suggest that rAAV2-retro particles in the blood can also diffuse into the cerebrospinal fluid and extensively transduce neurons in the spinal cord. There was no ipsilateral bias of neurons in the spinal cord after intraventricular injection or intravenous injection (Figure 6I). Compared to intravenous or intraventricular injections, more neurons in ipsilateral spinal cord were transduced after intramuscular injections (Figure 6J). This difference is mainly located in the cervical and thoracic vertebrae (Figure 6K). These results suggest that after intramuscular injection, the possible pathways for rAAV2-retro virus to extensively transduce neurons in the spinal cord include (1) diffusion through the spinal nerve into the cerebrospinal fluid, and (2) diffusion into the bloodstream and then uptake by the cerebrospinal fluid. Both pathways act simultaneously, allowing rAAV2-retro to spread out in the cerebrospinal fluid and extensively transduce neurons in the spinal cord.

DISCUSSION

Vector administration by intramuscular injections is minimally invasive and therefore constitutes a clinically relevant way of delivering therapeutic genes to the spinal cord.[26] As rAAV2-retro has been reported to effectively retrogradely transduce projection neurons in the brain,[17] we analyzed the potential of rAAV2-retro to retrogradely deliver genes to lower motor neurons in the spinal cord after intramuscular injections in neonatal mice. Through tissue clearing, fluorescent imaging, and 3D reconstruction, we found that rAAV2-retro was broadly effective in transducing lower motor neurons in the ventral horn of the spinal cord and the motor nuclei of the brainstem by a single injection in a single muscle in neonatal mice. Furthermore, we revealed that the intramuscular delivery of rAAV2-retro to lower motor neurons yielded a high transduction efficiency (57.04% ± 4.01%). Finally, through a SCI model test, we confirmed that rAAV2-retro injected through muscle was spread by the cerebrospinal fluid pathway to achieve the extensive transduction of lower motor neurons. These data show an important advancement in the potential for retrograde delivery of genes by rAAV2-retro to systemic lower motor neurons following intramuscular injection.

Many motor neuron diseases, including spinal muscular atrophy (SMA), have been confirmed to be associated with genetic defects. Because of the lack of effective pharmacological treatments, gene therapy therefore holds promise for the treatment of motor neuron diseases. However, widespread gene transfer to lower motor neurons is challenging. The main methods of gene transfer involve delivery to the cerebrospinal fluid (intracerebroventricular, intracisternal, and intrathecal routes), to the bloodstream (intravenous route) or to the muscle (intramuscular route).[27] Intravenous injections require high doses and high titers of rAAV and are inefficient. Unlike intracerebro-

ventricular, intracisternal, and intrathecal administration, which require stringent technical conditions, intramuscular administration is minimally invasive and thus constitutes a more clinically relevant pathway to deliver therapeutic genes to lower motor neurons. Moreover, lower motor neurons directly project to muscles, and intramuscular injection is considered the most specific and ideal approach for rAAV gene therapy in lower motor neuron diseases.[10,28] It relies on the ability of the rAAV to hijack the axonal transport pathway and travel along the nerve in a centripetal direction. Prior works have already revealed that some rAAV serotypes yield the effective transduction of cells in the spinal cord following intramuscular injection, but the efficiency of intramuscular injection for gene therapy is a limitation compared that of with intracerebroventricular, intracisternal, and intrathecal routes.[8–11,13,27,29] Here, we found that the injection of rAAV2-retro into the right forelimb *extensor carpi radialis* of P4 mice transduced the lower motor neurons projecting to the injected muscle with 57.04% efficiency when normalized to CTB-647 and mediated the most efficient retrograde transport among all tested rAAV serotypes. It has been reported that targeting at least 20%–40% of the motor neurons in the spinal cord is capable of producing substantial therapeutic effects in SMA mice, with a maximum therapeutic benefit when more than 50% of neurons are targeted.[6] These results show that the intramuscular injection of rAAV2-retro has the potential to produce considerable therapeutic effects in lower motor neuron diseases. Furthermore, our data also showed that a single administration of rAAV2-retro in a single muscle mediated the extensive transduction of lower motor neurons in the bilateral ventral horn of the spinal cord and in some motor nuclei of the brainstem. As gene-deficiency diseases, lesions of the lower motor neurons are usually widespread, so the rAAV2-retro-mediated extensive transduction of motor neurons may alleviate systemic symptoms.[30] Importantly, our data suggest that the cells transduced with rAAV2-retro in the spinal cord and brainstem are limited to ChAT-positive lower motor neurons. Although some neurons were not located in the ventral horn, they were invariably identified as ChAT-positive (Figure S4A). Such extensive and specific expression is of vast significance, as a single intramuscular injection of rAAV2-retro can extensively deliver genes to the lower motor neurons of the whole spinal cord and brainstem to treat multiple muscles while avoiding transgene upregulation in nontargeted cells, thus preventing deleterious side effects. Meanwhile, DRG neurons are extensively transduced (Figure S5). Therefore, the neurons that are transduced have the property of projecting to the muscles. We speculate that this may be related to the serotype characteristics of rAAV2-retro, which are swallowed by neurons from the distal end, but more experiments are needed to provide evidence. Taken together, these findings provide a basis for the intramuscular injection of rAAV2-retro as a simple and practical therapeutic gene delivery method to extensively transduce lower motor neurons in the spinal cord and brainstem.

The route of muscle administration largely determines which cells are exposed to rAAV2-retro and hence limits potential transduction to only those cells. Unexpectedly, we observed that rAAV2-retro mediates extensive lower motor neuron transduction in the spinal cord

and brainstem, while CTB-647 only transduces the lower motor neurons projecting to the injected muscle. Based on previous observations, it is possible to achieve the retrograde transduction of rAAV2-retro directly through neuronal axons, through the bloodstream, or through uptake into the cerebrospinal fluid at neuromuscular junctions.[8,13] Our data strongly support a retrograde transport mechanism for the transduction of neurons that project to the injected muscle (Figure 5). However, how rAAV2-retro extensively transduces neurons that do not directly project to the injected muscle needs to be further determined. By PCR analysis, we found rAAV2-retro viral particles in cerebrospinal fluid and blood after intramuscular injection. A previous study speculated that scAAV9 may spread into the bloodstream after intramuscular injection.[8] However, we observed that, although rAAV2-retro extensively transduces cells in the CNS following intramuscular injection, the transduced cells were all ChAT-positive motor neurons, and DRG cells are also globally transduced at the same time. So, we think that the transduction after intramuscular injection could be achieved by spreading through the cerebrospinal fluid. To confirm this, we performed SCI before intramuscular injection to block cerebrospinal fluid circulation in the spinal cord, which did not affect blood circulation. The results showed that the SCI group exhibited a disrupted the pattern of rAAV2-retro transduction. This suggests that rAAV2-retro rely on cerebrospinal fluid circulation to achieve the extensive transduction of motor neurons after intramuscular injection. Similarly, cells in the spinal cord were extensively transduced after intraventricular injection. Because neurons in the ipsilateral thoracic segments near the lumbar spine can still be strongly transduced after SCI, we hypothesized that rAAV2-retro could be taken up by the cerebrospinal fluid through the spinal nerves. In addition, extensive transduction of cells in the spinal cord was found after intravascular injection. This indicates that rAAV2-retro can be absorbed by the cerebrospinal fluid through the blood vessels after intramuscular injection. Therefore, we speculate that there are two pathways for rAAV2-retro virus to extensively transduce neurons in the spinal cord after intramuscular injection: (1) diffusion through the spinal nerve into the cerebrospinal fluid, and (2) diffusion into the bloodstream and then uptake by the cerebrospinal fluid. Both pathways act simultaneously, allowing rAAV2-retro to spread out in the cerebrospinal fluid and extensively transduce neurons in the spinal cord. However, the mechanism by which the rAAV2-retro vector is taken up into the cerebrospinal fluid directly or into the blood after intramuscular injection needs to be studied further. Although intramuscular and intravascular injections are commonly used in clinically peripheral administration, intramuscular injections can achieve more neuronal transduction in the spinal cord at the same dose of rAAV2-retro (Table S2; Figures 6J and 6K). Therefore, intramuscular injection may be more advantageous than intravascular injection in treating related diseases.

In summary, gene delivery by the intramuscular injection of rAAV2-retro represents a promising tool for the study of neuroanatomy and disease. The selective, extensive, and highly efficient transduction of lower motor neurons observed creates opportunities for a number of novel studies. The targeted delivery to and the expression of therapeutic genes in specific cell populations are key requirements of gene therapy, especially in the CNS. Given the importance of motor neurons in neuromuscular diseases, these findings with regard to rAAV2-retro may have therapeutic implications for motor neuron diseases such as SMA. However, it is unclear whether rAAV2-retro serotype can be used in other species therapeutically, including humans, and more tests are needed to prove that rAAV2-retro has wide species tropism.

MATERIALS AND METHODS

Animals

All procedures were in accordance with protocols approved by the Hubei Provincial Animal Care and Use Committee and the guidelines of the Animal Experimentation Ethics Committee of Huazhong University of Science and Technology. C57BL/6J mice were purchased from Beijing Vital River (Beijing, China). All animals were group-housed with their littermates in a dedicated housing room under a 12-h light/12-h dark cycle, and food and water were available *ad libitum.*

rAAV Vectors

rAAV serotypes (rAAV1, rAAV2, rAAV5, rAAV6, rAAV7, rAAV8, rAAV9, and rAAV2-retro) were purchased from Vigene Biosciences (Jinan, China). Each of the viral constructs was generated by the assembly of viral genomes expressing viral proteins and containing an enhanced GFP or a RFP transgene using the triple plasmid transfection of HEK293 cells, as described previously.[31] The pAV-MIR-GFP plasmid contained two wild-type rAAV2 terminal repeats, a short hairpin (shRNA) insertion site under the control of the pUC promoter, a sequence encoding GFP driven by the CMV promoter, a human β-globin intron, and the ampicillin resistance gene. Separate Rep/Cap plasmids and a helper plasmid containing the components of the viral replication machinery and the capsid proteins of selected rAAV serotypes were cotransfected into HEK293 cells. After the HEK293 cells were lysed, the rAAV particles were purified by iodixanol gradient ultracentrifugation. Viral titers were determined by qPCR.

Injection of the rAAV Serotypes

Hypothermic anesthesia was induced in mice on P4 by aluminum plates cooled on ice, as described previously.[32] For intramuscular injection, the *extensor carpi* muscle was exposed by making an incision between the elbow and wrist of the lower right forelimb. The viruses were diluted in a stroke-physiological saline solution to a final titer of 5.0×10^{12} genome copies/mL prior to injection. A total of 1.25×10^{10} viral particles (2.5 µL) of rAAV-CMV-GFP (rAAV1, rAAV2, rAAV5, rAAV6, rAAV7, rAAV8, rAAV9, and rAAV2-retro, n = 4 for each group) were unilaterally injected into one site of the *extensor carpi* muscle of the right forelimb of each P4 pup using a glass micropipette connected to a syringe pump (item no. 53311, Quintessential Stereotaxic Injector, Stoelting, Wood Dale, IL, USA). Each rAAV serotype was unilaterally injected into four animals at a rate of 0.8 µL/min, with the micropipette being held in place for an additional 30 s after injection before being slowly retracted from the muscle. To

reconstruct the three-dimensional distribution of the rAAV2-retro-transduced cells, 2.5 μL of rAAV2-retro particles (a final titer of 1.0×10^{13} genome copies/mL) or 0.5 μL of rAAV2-retro particles (a final titer of 1.0×10^{14} genome copies/mL) in sterile 0.9% NaCl was injected into the *extensor carpi* or gastrocnemius muscle of P4 neonatal mice. To quantify the transduction efficiency, rAAV2-retro particles (a final titer of 1.0×10^{13} genome copies/mL) were mixed with CTB-647 (C34778, Thermo Fisher Scientific, a final concentration of 1%) in sterile 0.9% NaCl, and 2.5 μL of the mixture was injected into the *extensor carpi* muscle of P4 neonatal mice. For intraventricular injection, the P4 mice were gently attached to a stereotaxic instrument after anesthesia. We made sure the head was horizontal on the y axis (from front to back) by checking the line between lambda and bregma, and horizontal on the x axis (from side to side) by checking the line between the eyes. The stereotaxic manipulator was used to position the micropipette above lambda and then zero for the X and Y coordinates and then move the stereotaxic arms to (X, Y) = (0.85, 1.55) mm. 0.5 μL of rAAV2-retro particles (a final titer of 1.0×10^{14} genome copies/mL) in sterile 0.9% NaCl was loaded into the micropipette. The micropipette was inserted until Z = −1.7 mm and then retracted to −1.5 mm. rAAV particles were injected into ventricle at a rate of 0.8 μL/min, with the micropipette being held in place for an additional 30 s after injection before being slowly retracted. For intravenous injection, 0.5 μL of rAAV2-retro particles (a final titer of 1.0×10^{14} genome copies/mL) in sterile 0.9% NaCl was placed on Parafilm and subsequently drawn into 1-mL insulin syringes with 29-gauge needles. A light microscope was used to visualize the temporal vein, and the needle was inserted into the veins of P4 neonatal mice, followed by manually depressing the plunger with the needle being held in place for an additional 30 s to prevent backflow of the injectant. After a proper injection, the mice were rubbed with bedding to prevent rejection by the mother and then returned to their cage. An overview of animal numbers and experimental variables is provided in Table S1.

Tissue Preparation and Imaging

The animals were transcardially perfused with 0.01 M PBS followed by 4% paraformaldehyde (PFA) in 0.01 M PBS (pH 7.4). The cervical segments of the mouse spinal cord were carefully removed and postfixed in 4% PFA overnight at 4°C, washed three times in PBS, and stored in PBS. Agarose embedding was performed as described previously.[33,34] Briefly, agarose type IA (A0169, Sigma-Aldrich) was oxidized by stirring in a 10 mM sodium periodate ($NaIO_4$, S1878, Sigma-Aldrich) solution for 2 h at room temperature, washed three times, and resuspended in 0.01 M PBS to reach a final concentration of 6%. The spinal cords were washed with 0.01 M PBS three times after postfixation and embedded in melted 6% agarose using a silicone cube-shaped mold. The silicone mold was cooled at room temperature until the agarose was completely solidified. Covalent cross-linking between the spinal cord surface and the agarose was activated by equilibration in an excess of 0.2% (w/v) sodium borohydride ($NaBH_4$, 452882, Sigma-Aldrich) in 0.05 M sodium borate buffer (pH 9.0–9.5) overnight at 4°C. Sodium borohydride buffer was freshly prepared overnight. Transverse sections (50 mm) of the cervical spinal cord

were prepared using a Vibratome (Leica VT1200 S, Leica Microsystems). Each section was visualized with a slide scanning microscope (Ni-E, Nikon). For the quantitative analysis of *in vivo* viral transduction, labeled cells with well-defined soma area were counted on every second serial section and corrected using Abercrombie's formula to compensate for double counting of profiles: N = T/(T + D) × 2n, where N is the corrected number of cells, T is the thickness of the section, D is the mean diameter of 10 nuclei, and n is the number of counted nuclei.[35] The diameter of the soma of the labeled cells was measured using ImageJ.

Tissue Clearing and Imaging

The animals were transcardially perfused with 0.01 M PBS followed by 4% PFA in 0.01 M PBS (pH 7.4). The intact brains and spinal cords were carefully dissected and postfixed in 4% PFA overnight at 4°C, washed three times in PBS, and stored in PBS. A FDISCO clearing procedure was used to process the samples according to the process described in the original paper; the procedure included two steps: dehydration and refractive index matching.[36] Briefly, the samples were incubated with peroxide-free tetrahydrofuran (THF, 186562, Sigma-Aldrich) solutions (mixed with distilled H_2O [dH_2O], 50%, 70%, 80%, and 100% trimethylamine, pH adjusted to 9.0, T103287, Aladdin Reagent, Shanghai, China) on a shaker at 4°C. After dehydration, the samples were transferred to a pure dibenzyl ether (DBE) solution (108014, Sigma-Aldrich) for refractive index matching. The peroxides in THF and DBE were removed by passing 100% THF through a chromatography column filled with basic activated aluminum oxide (20001861, Sinopharm Chemical Reagent, Shanghai, China), as previously described.[37,38] The clearing agent was freshly prepared, and the incubation time for each step was determined by the tissue type, according to the original paper. The spinal cords mounted on glass coverslips and incubated in DBE were imaged using an inverted confocal fluorescence microscope (LSM 710, Zeiss) equipped with a 10× Fluor objective (numerical aperture [NA], 0.50, dry; working distance, 2.0 mm) and a 20× Plan Apochromatic objective (NA, 0.80, dry; working distance, 0.55 mm). The z-step interval was 5–9 μm. The brains incubated in DBE were imaged using a light sheet fluorescence microscope (Ultramicroscope, LaVision Bio-Tec, Göttingen, Germany) equipped with a 2× Plan Apochromatic zoom objective (NA, 0.50). The z-step interval was 10 μm. The analysis and 3D reconstructions of the obtained images were performed with ImageJ and Imaris software. The locations and counts of cells in the spinal cord (Figures 2, 5, and 6) were determined by the "Spots" function of Imaris. A summary of statistical results is provided in Tables S2 and S3. The surface of spinal cord was refactored by the "Surfaces" function of Imaris. Videos were generated using Imaris.

Immunostaining

Transverse sections of the cervical spinal cord were immunolabeled for ChAT. The sections were blocked with 10% rabbit serum in 0.01 M PBS and 0.3% Triton X-100 for 1 h at room temperature before staining. The floating sections were incubated with a primary goat anti-ChAT polyclonal antibody (AB144P, 1:250, EMD Millipore) at 4°C overnight and washed three times for 10 min with

0.01 M PBS before incubation with a secondary antibody (A-11012, 1:500, Invitrogen) and NeuroTrace Blue Nissl (N21479, 1:200, Invitrogen) or DAPI (10236276001, 1:100,000, Roche) for 2 h at room temperature. After thorough washing with 0.01 M PBS, the sections were mounted with an antifluorescence quenching agent for imaging and analysis. Then, the sections were imaged with an LSM 710 inverted confocal fluorescence microscope.

Spinal Cord Transection Injury

After hypothermic anesthesia and local anesthesia with lidocaine, a laminectomy was performed to expose one to two segments of spinal segments T9–T11 under microscopic control. Spinal cord transection injury was generated using a microscopic shear to completely cut the entire spinal cord. Sterile cotton swabs were used to drain the leaking cerebrospinal fluid and blood and apply pressure to stop bleeding. The skin incision was closed with a sterile 6.0 suture and a needle holder. The sham group was sutured without cutting the spinal cord. After surgery, the mice were returned to their cages in preparation for the injection.

Histological Outcomes after Spinal Cord Transection Injury

To analyze histological outcomes after spinal cord transection injury, mice were sacrificed 7 d after the injury. After cryoprotection in 30% sucrose at 4°C for 2 d, spinal cords were sectioned (30 μm) encompassing the injury epicenter. The selected sections were stained with a H&E staining kit (E607318, Sangon Biotech, Shanghai, China) and imaged with a slide scanning microscope (Ni-E, Nikon).

Cerebrospinal Fluid/Blood Isolation and PCR

To extract the cerebrospinal fluid containing rAAV2-retro particles, the *dura mater* of the thoracic vertebrae was first exposed, and the cerebrospinal fluid was collected with a pipette after gently piercing the *dura mater* with an insulin needle (29G) 3 h after intramuscular injection. Blood was collected directly from the heart with a new insulin needle. Five microliters of cerebrospinal fluid or blood from the mice injected with rAAV2-retro, a virus solution of rAAV2-retro particles as a positive control, or cerebrospinal fluid of the mice injected with sterile physiological saline as a negative control was mixed with 4 μL of sterile physiological saline and 1 μL proteinase K (10 μg/μL). The mixtures were incubated in a 37°C water bath for 30 min and incubated at 95°C for 10 min to inactivate the proteinase K. The rAAV2-retro particles were identified by PCR (annealing temperature 60°C) using GFP forward and reverse primers (5′-CTGGTCGAGCTGGACGGCGACG-3′ and 5′-CACGAACTCCAGCAGGACCATG-3′, respectively) for rAAV2-retro-CMV-GFP or RFP forward and reverse primers (5′-CATGGAGGGCTCCGTGAAC-3′ and 5′-CGATGGTGTAGTCCTCGTTGTG-3′, respectively) for rAAV2-retro-CMV-RFP. Genomic DNA extracted from rAAV2-retro was amplified in a 20-μL reaction volume under the following conditions: 94°C for 3 min; 35 cycles at 94°C for 30 s, 60°C for 30 s, and 72°C for 30 s; and a final extension step at 72°C for 5 min. The gel images were digitized using a Bio-Rad imager (Bio-Rad ChemiDoc MP, Bio-Rad). Amplified product bands of 630 and 581 bp were observed by agarose gel electrophoresis for rAAV2-retro-CMV-GFP and rAAV2-retro-CMV-RFP, respectively.

Statistical Analysis

Data analyses and graph construction were performed using SPSS (version 13.0) and R (version 3.5.3) software. The results are displayed as the means ± SEM. For statistical analyses, two-tailed unpaired t tests or one-way ANOVA followed by the Bonferroni correction were performed. The p values were calculated using an independent-sample t test (two-sided) to compare the data between the two groups. One-way ANOVA was used to compare more than two groups of data. In this study, $p < 0.05$ was considered significant (*$p < 0.05$, **$p < 0.01$, and ***$p < 0.001$).

SUPPLEMENTAL INFORMATION

Supplemental Information can be found online at https://doi.org/10.1016/j.omtm.2019.11.006.

REFERENCES

1. Stifani, N. (2014). Motor neurons and the generation of spinal motor neuron diversity. Front. Cell. Neurosci. 8, 293.

2. Arber, S. (2012). Motor circuits in action: specification, connectivity, and function. Neuron 74, 975–989.

3. Sherrington, C. (1952). The Integrative Action of the Nervous System (Cambridge University Press Archive).

4. Kania, A. (2014). Spinal motor neuron migration and the significance of topographic organization in the nervous system. Adv. Exp. Med. Biol. 800, 133–148.

5. Yamazaki, T., Chen, S., Yu, Y., Yan, B., Haertlein, T.C., Carrasco, M.A., Tapia, J.C., Zhai, B., Das, R., Lalancette-Hebert, M., et al. (2012). FUS-SMN protein interactions link the motor neuron diseases ALS and SMA. Cell Rep 2, 799–806.

6. Meyer, K., Ferraiuolo, L., Schmelzer, L., Braun, L., McGovern, V., Likhite, S., Michels, O., Govoni, A., Fitzgerald, J., Morales, P., et al. (2015). Improving single injection CSF delivery of AAV9-mediated gene therapy for SMA: a dose–response study in mice and nonhuman primates. Mol. Ther 23, 477–487.

7. Bucher, T., Colle, M.A., Wakeling, E., Dubreil, L., Fyfe, J., Briot-Nivard, D., Maquigneau, M., Raoul, S., Cherel, Y., Astord, S., et al. (2013). scAAV9 intracisternal

delivery results in efficient gene transfer to the central nervous system of a feline model of motor neuron disease. Hum. Gene Ther. *24*, 670–682.

8. Benkhelifa-Ziyyat, S., Besse, A., Roda, M., Duque, S., Astord, S., Carcenac, R., Marais, T., and Barkats, M. (2013). Intramuscular scAAV9-SMN injection mediates widespread gene delivery to the spinal cord and decreases disease severity in SMA mice. Mol. Ther. *21*, 282–290.

9. Hardcastle, N., Boulis, N.M., and Federici, T. (2018). AAV gene delivery to the spinal cord: serotypes, methods, candidate diseases, and clinical trials. Expert Opin. Biol. Ther. *18*, 293–307.

10. Towne, C., Schneider, B.L., Kieran, D., Redmond, D.E., Jr., and Aebischer, P. (2010). Efficient transduction of non-human primate motor neurons after intramuscular delivery of recombinant AAV serotype 6. Gene Ther. *17*, 141–146.

11. Hollis Ii, E.R., Kadoya, K., Hirsch, M., Samulski, R.J., and Tuszynski, M.H. (2008). Efficient Retrograde Neuronal Transduction Utilizing Self-complementary AAV1. Mol. Ther. *16*, 296–301.

12. Tosolini, A.P., and Morris, R. (2016). Targeting motor end plates for delivery of adenoviruses: an approach to maximize uptake and transduction of spinal cord motor neurons. Sci. Rep. *6*, 33058.

13. Ayers, J.I., Fromholt, S., Sinyavskaya, O., Siemienski, Z., Rosario, A.M., Li, A., Crosby, K.W., Cruz, P.E., DiNunno, N.M., Janus, C., et al. (2015). Widespread and efficient transduction of spinal cord and brain following neonatal AAV injection and potential disease modifying effect in ALS mice. Mol. Ther. *23*, 53–62.

14. Daya, S., and Berns, K.I. (2008). Gene therapy using adeno-associated virus vectors. Clin. Microbiol. Rev. *21*, 583–593.

15. Mendell, J. (2014). Gene transfer clinical trial for spinal muscular atrophy type 1. ClinicalTrials.gov: NCT02122952, https://clinicaltrials.gov/ct2/show/NCT02122952

16. Bonnemann, C. (2015). Intrathecal administration of scAAV9/JeT-GAN for the treatment of giant axonal neuropathy. ClinicalTrials.gov: NCT02362438, https://clinicaltrials.gov/ct2/show/NCT02362438.

17. Tervo, D.G., Hwang, B.Y., Viswanathan, S., Gaj, T., Lavzin, M., Ritola, K.D., Lindo, S., Michael, S., Kuleshova, E., Ojala, D., et al. (2016). A designer AAV variant permits efficient retrograde access to projection neurons. Neuron *92*, 372–382.

18. Klug, J.R., Engelhardt, M.D., Cadman, C.N., Li, H., Smith, J.B., Ayala, S., Williams, E.W., Hoffman, H., and Jin, X. (2018). Differential inputs to striatal cholinergic and parvalbumin interneurons imply functional distinctions. eLife *7*, e35657.

19. Wang, Z., Maunze, B., Wang, Y., Tsoulfas, P., and Blackmore, M.G. (2018). Global connectivity and function of descending spinal input revealed by 3D microscopy and retrograde transduction. J. Neurosci. *38*, 10566–10581.

20. Walji, A.H., and Tsui, B.C. (2016). Clinical anatomy of the brachial plexus. In Pediatric Atlas of Ultrasound- and Nerve Stimulation-Guided Regional Anesthesia, B. Tsui and S. Suresh, eds. (Springer), pp. 149–163.

21. al-Qattan, M.M. (1996). The nerve supply to extensor carpi radialis brevis. J. Anat. *188*, 249–250.

22. Tosolini, A.P., Mohan, R., and Morris, R. (2013). Targeting the full length of the motor end plate regions in the mouse forelimb increases the uptake of fluoro-gold into corresponding spinal cord motor neurons. Front. Neurol. *4*, 58.

23. Mohan, R., Tosolini, A.P., and Morris, R. (2014). Targeting the motor end plates in the mouse hindlimb gives access to a greater number of spinal cord motor neurons: an approach to maximize retrograde transport. Neuroscience *274*, 318–330.

24. Spiller, K.J., Khan, T., Dominique, M.A., Restrepo, C.R., Cotton-Samuel, D., Levitan, M., Jafar-Nejad, P., Zhang, B., Soriano, A., Rigo, F., et al. (2019). Reduction of matrix metalloproteinase 9 (MMP-9) protects motor neurons from TDP-43-triggered death in rNLS8 mice. Neurobiol. Dis. *124*, 133–140.

25. Tang, X., Büttner-Ennever, J.A., Mustari, M.J., and Horn, A.K. (2015). Internal organization of medial rectus and inferior rectus muscle neurons in the C group of the oculomotor nucleus in monkey. J. Comp. Neurol. *523*, 1809–1823.

26. Tosolini, A.P., and Morris, R. (2016). Viral-mediated gene therapy for spinal cord injury (SCI) from a translational neuroanatomical perspective. Neural Regen. Res. *11*, 743–744.

27. Hudry, E., and Vandenberghe, L.H. (2019). Therapeutic AAV gene transfer to the nervous system: a clinical reality. Neuron *101*, 839–862.

28. Boulis, N.M., Noordmans, A.J., Song, D.K., Imperiale, M.J., Rubin, A., Leone, P., During, M., and Feldman, E.L. (2003). Adeno-associated viral vector gene expression in the adult rat spinal cord following remote vector delivery. Neurobiol. Dis. *14*, 535–541.

29. Saraiva, J., Nobre, R.J., and Pereira de Almeida, L. (2016). Gene therapy for the CNS using AAVs: the impact of systemic delivery by AAV9. J. Control. Release *241*, 94–109.

30. Stephens, B., Guiloff, R.J., Navarrete, R., Newman, P., Nikhar, N., and Lewis, P. (2006). Widespread loss of neuronal populations in the spinal ventral horn in sporadic motor neuron disease. a morphometric study. J. Neurol. Sci. *244*, 41–58.

31. Schober, A.L., Gagarkin, D.A., Chen, Y., Gao, G., Jacobson, L., and Mongin, A.A. (2016). Recombinant adeno-associated virus serotype 6 (rAAV6) potently and preferentially transduces rat astrocytes *in vitro* and *in vivo*. Front. Cell. Neurosci. *10*, 262.

32. Kim, J.Y., Grunke, S.D., Levites, Y., Golde, T.E., and Jankowsky, J.L. (2014). Intracerebroventricular viral injection of the neonatal mouse brain for persistent and widespread neuronal transduction. J. Vis. Exp. (91), 51863.

33. Jiang, T., Long, B., Gong, H., Xu, T., Li, X., Duan, Z., Li, A., Deng, L., Zhong, Q., Peng, X., and Yuan, J. (2017). A platform for efficient identification of molecular phenotypes of brain-wide neural circuits. Sci. Rep. *7*, 13891.

34. Ragan, T., Kadiri, L.R., Venkataraju, K.U., Bahlmann, K., Sutin, J., Taranda, J., Arganda-Carreras, I., Kim, Y., Seung, H.S., and Osten, P. (2012). Serial two-photon tomography for automated ex vivo mouse brain imaging. Nat. Methods *9*, 255–258.

35. Bácskai, T., Fu, Y., Sengul, G., Rusznák, Z., Paxinos, G., and Watson, C. (2013). Musculotopic organization of the motor neurons supplying forelimb and shoulder girdle muscles in the mouse. Brain Struct. Funct. *218*, 221–238.

36. Qi, Y., Yu, T., Xu, J., Wan, P., Ma, Y., Zhu, J., Li, Y., Gong, H., Luo, Q., and Zhu, D. (2019). FDISCO: advanced solvent-based clearing method for imaging whole organs. Sci. Adv *5*, eaau8355.

37. Ertürk, A., Becker, K., Jährling, N., Mauch, C.P., Hojer, C.D., Egen, J.G., Hellal, F., Bradke, F., Sheng, M., and Dodt, H.U. (2012). Three-dimensional imaging of solvent-cleared organs using 3DISCO. Nat. Protoc. *7*, 1983–1995.

38. Becker, K., Jährling, N., Saghafi, S., Weiler, R., and Dodt, H.U. (2012). Chemical clearing and dehydration of GFP expressing mouse brains. PLoS ONE *7*, e33916.